PUBLICATION I

Comparison of substrate specificity of tyrosinases from *Trichoderma reesei* and *Agaricus bisporus*

In: Enzyme and Microbial Technology 44(2009),
pp. 1–10.

Enzyme and Microbial Technology 44 (2009) 1–10

Contents lists available at ScienceDirect

Enzyme and Microbial Technology

journal homepage: www.elsevier.com/locate/emt

Comparison of substrate specificity of tyrosinases from *Trichoderma reesei* and *Agaricus bisporus*

Emilia Selinheimo[a,*], Chiara Gasparetti[a], Maija-Liisa Mattinen[a], Charlotte L. Steffensen[b], Johanna Buchert[a], Kristiina Kruus[a]

[a] VTT Technical Research Centre of Finland, P.O. Box 1000, Espoo FIN-02044 VTT, Finland
[b] Department of Food Science, Faculty of Agricultural Sciences, Aarhus University, Research Centre Foulum, P.O. Box 50, DK-8830 Tjele, Denmark

ARTICLE INFO

Article history:
Received 5 May 2008
Received in revised form 4 September 2008
Accepted 26 September 2008

Keywords:
Tyrosinase
Fungal
Substrate specificity
Kinetic constants

ABSTRACT

Understanding the substrate specificity of tyrosinases (EC 1.14.18.1) as well as their capability to oxidize peptide-bound tyrosine residues is important in a view of applicability of tyrosinases. In the present study, two fungal tyrosinases, an extracellular enzyme from the filamentous fungus *Trichoderma reesei* (TrT) and an intracellular enzyme from the edible mushroom *Agaricus bisporus* (AbT) were compared. Oxidation of various mono- and diphenolic compounds and tyrosine-containing tripeptides was examined and kinetic constants determined using spectrophotometric and oxygen consumption measurements. TrT and AbT were found to show notable differences in their substrate specificity. TrT generally showed 10-fold higher K_m values than AbT. The presence of a carboxylic and amine group in the substrate influenced the enzymes differently. While the substrates with a carboxyl group were observed not to be effectively oxidized by AbT, the amine group seemed to hider the oxidation in the TrT-catalyzed reactions. Moreover, the UV–visible absorption spectra on the oxidation of catechol and hydrocaffeic acid showed that the product patterns were different between the enzymes. The result is interesting as the primary products from tyrosinase-catalyzed reactions were assumed to be identical with both enzymes. Furthermore, a nucleophilic 3-methyl-2-benzothiazolinone hydrazone (MBTH) affected differently on the activity of the tyrosinases: the lag period related to the oxidation of monophenols was prolonged by MBTH with TrT, whereas with AbT the lag was shortened.

1. Introduction

Tyrosinases (monophenol, *o*-diphenol:oxygen oxidoreductase, EC 1.14.18.1) are copper-containing metalloproteins and widely found in microbes, plants and mammals. These enzymes are known as type 3 copper proteins having a diamagnetic spin-coupled copper pair in the active centre [1]. Tyrosinases catalyze the *o*-hydroxylation of monophenols and subsequent oxidation of *o*-diphenols to quinones [2,3]. Molecular oxygen is used as an electron acceptor in the catalysis, with subsequent reduction of oxygen to water. The binuclear active site of tyrosinases is known to exist in three states: *oxy*-tyrosinase, *met*-tyrosinase and *deoxy*-tyrosinase. Both *met*- and *oxy*-states of tyrosinases can catalyze diphenolase reaction, whereas the hydroxylation reaction that is involved in the monophenolase catalytic cycle requires the *oxy*-form of the active site, in which dioxygen is bound as a peroxide [7,8]. *Deoxy*-tyrosinase is a reduced and instable form and binds oxygen to give the *oxy*-form [4–6].

Even though many tyrosinase proteins and the corresponding genes have been characterized from bacteria, fungi, plants and mammals, the protein structures of the different tyrosinases are still largely unrevealed. However, the crystal structure of the *Streptomyces castaneoglobisporus* tyrosinase was recently resolved [8]. The *S. castaneoglobisporus* tyrosinase was shown to have similarities with the crystal structures of the catechol oxidase from *Ipomoea batatas* [9] and hemocyanin, an oxygen carrier protein from *Octopus dofleini* [10]. Furthermore, the identical catalytic mechanism between the tyrosinases of different origin has been postulated [8,11,12].

Characteristics of various fungal tyrosinases, especially the enzymes from *Agaricus bisporus* [13,14] and *Neurospora crassa* [2], have been investigated comprehensively. The fungal tyrosinase from the edible mushroom *A. bisporus* (AbT) [13,15,16] is reported to be composed of two monomeric subunits [13,14]. Based on the

Abbreviations: TrT, tyrosinase from *Trichoderma reesei*; AbT, tyrosinase from *Agaricus bisporus*; Y, tyrosine; G, glycine; MBTH, 3-methyl-2-benzothiazolinone hydrazone; [S], substrate concentration.

* Corresponding author at: P.O. Box 1500, Espoo FIN-02044 VTT, Finland. Tel.: +358 20 722 7135 fax: +358 20 722 7071.
E-mail address: emilia.selinheimo@vtt.fi (E. Selinheimo).

0141-0229/$ – see front matter © 2008 Elsevier Inc. All rights reserved.
doi:10.1016/j.enzmictec.2008.09.013

cDNAs the predicted molecular weight of AbT is 64 kDa. The mature protein, however, show a molecular mass of 43 kDa with a putative cleavage site in the C-terminus [14]. Recently Selinheimo et al. [17] reported the production and purification of a novel tyrosinase from *Trichoderma reesei* (TrT). Similarly to AbT, the mature protein of TrT was processed from C-terminus and TrT showed a molecular mass of 43.2 kDa [17]. Unlike the intracellular plant, fungal and animal tyrosinases studied thus far, the gene *tyr2* of *T. reesei* was found to contain a signal sequence, and the gene product was verified to be secreted. Moreover, the extracellular TrT enzyme was produced at high amount, which is rather exceptional within this class of enzymes. The tyrosinases from *Gibberella zeae*, *N. crassa* and *Magnaporthe grisea* also contain putative signal sequences, suggesting extracellular enzymes [17]. However, they have not been characterized at a protein level. The reported *Streptomyces* tyrosinases are also secreted, but the secretion of the bacterial tyrosinases is assisted by another protein, which has a signal sequence [18,19].

Comparison of biochemical characteristics of the intracellular AbT and the extracellular TrT has recently been performed by Selinheimo et al. [20]. AbT and TrT were found to differ, especially, in their protein crosslinking ability, and in the efficiency to oxidize substrates substituted with amine and carboxyl acid group [20]. In the present study, the aim was to further elucidate the influence of the substitution of mono- and diphenolic compounds on the affinity and the catalytic efficiency of AbT and TrT.

2. Materials and methods

2.1. Enzymes

TrT was produced, purified as described by Selinheimo et al. [17]. AbT was obtained from Fluka, and it was dissolved in 0.1 M sodium phosphate buffer, pH 7.0. For some experiments, AbT was further purified as described by Duckworth and Coleman [21].

2.2. Chemicals

L-Tyrosine, 3,4-dihydroxy-L-phenylalanine (L-dopa), L-tyramine, L-dopamine, *p*-coumaric acid, were from Sigma, *p*-tyrosol 3-(4-hydroxyphenyl)propanoic acid (phloretic acid) and 3-(3,4-dihydroxyphenyl)propanoic acid (hydrocaffeic acid) were from Aldrich, caffeic acid and pyrocatechol were from Fluka, phenol and benzoic acid were from Merck, and the peptides glycine-glycine-tyrosine (GGY), glycine-tyrosine-glycine (GYG) and tyrosine-glycine-glycine (YGG) from Bachem. 3-methyl-2-benzothiazolinone hydrazone (MBTH) and aniline were from Sigma.

2.3. Enzyme activity assays

Tyrosinase activity was measured as described by Robb [3], with few modifications, using 15 mM L-dopa and 2 mM L-tyrosine as substrates. Activity assays were carried out in 0.1 M sodium phosphate buffer (pH 7.0) at 25 °C either by monitoring dopachrome formation at 475 nm ($\varepsilon_{\text{dopachrome}} = 3400\ \text{M}^{-1}\ \text{cm}^{-1}$) or by monitoring the consumption of the co-substrate oxygen, with a single channel fibre-optic oxygen meter for mini-sensors (Precision sensing GmbH, Regensburg, Germany). The oxygen consumption assay was performed as described by Selinheimo et al. [17]. Furthermore, the enzymatic activities on L-dopa (15 mM) and L-tyrosine (2 mM) were detected by a spectrophotometric assay in the presence of chromogenic nucleophile 3-methyl-2-benzothiazolinone hydrazone (MBTH). A coupling reaction between MBTH and *o*-quinones that are generated during the oxidation of monophenols and *o*-diphenols leads to the formation a MBTH-quinone adduct absorbing at 510 nm ($\varepsilon = 22\ 300\ \text{M}^{-1}\ \text{cm}^{-1}$) [22–25]. In the activity assay with MBTH, concentrations of 0.25–10 mM of MBTH were used, and 2% (v/v) *N*,*N*-dimethylformamide was added to the reaction mixture to keep the MBTH-quinone adducts in solution.

2.4. Determination of kinetic parameters K_m and V_{max}

Monophenolic compounds, L-tyrosine, phenol, L-tyramine, *p*-coumaric acid, phloretic acid and their corresponding diphenols L-dopa, catechol, L-dopamine, caffeic acid, hydrocaffeic acid, and additionally monophenolic *p*-tyrosol (Fig. 1), were dissolved at a concentration of 0.1–20 mM in 0.1 M sodium phosphate buffer (pH 7.0). TrT and AbT dosages per 1 ml of substrate were 3.8 and 3.1 μg for the monophenols and 0.9 and 0.8 μg for the diphenols, respectively. Kinetic assays were carried out by monitoring the enzymatic reactions by measuring the product formation at the selected wavelengths at 25 °C. Specific wavelengths for the product formation from substrates were determined according to the UV–visible absorption spectrum of the oxidation products from the particular substrates by the enzymes. Formation of the UV–visible absorption spectra were monitored as a function of enzyme reaction time. For the tripeptides, GGY, GYG and YGG, the kinetic constants were analyzed by the oxygen consumption assay. Peptides were dissolved in 0.1 M sodium phosphate buffer (pH 7), reaction volume was 1.8 ml, and TrT and AbT doses were 40 and 30 μg, respectively. Kinetic constants K_m, V_{max} and k_{cat} were obtained with the Graph Pad Prism 3.02 program (Graph Pad Software Inc., San Diego, CA, USA). Additionally, the absorption spectra of the oxidation products of the tripeptides by TrT and AbT were determined.

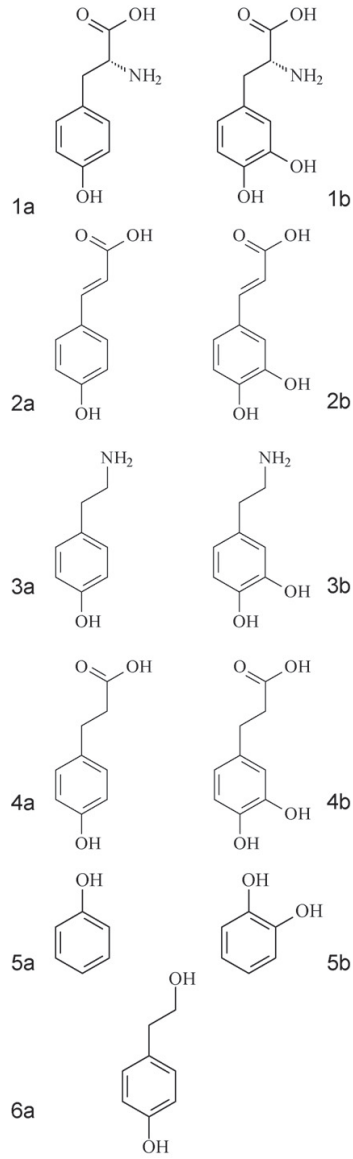

Fig. 1. Chemical structures of the substrates used in the study: **1a** L-tyrosine, **1b** L-dopa, **2a** *p*-coumaric acid, **2b** caffeic acid, **3a** L-tyramine, **3b** L-dopamine, **4a** 3-(4-hydroxyphenyl) propanoic acid (phloretic acid), **4b** 3,4-dyhydroxycinnamic acid (hydrocaffeic acid), **5a** phenol, **5b** catechol, **6a** *p*-tyrosol.

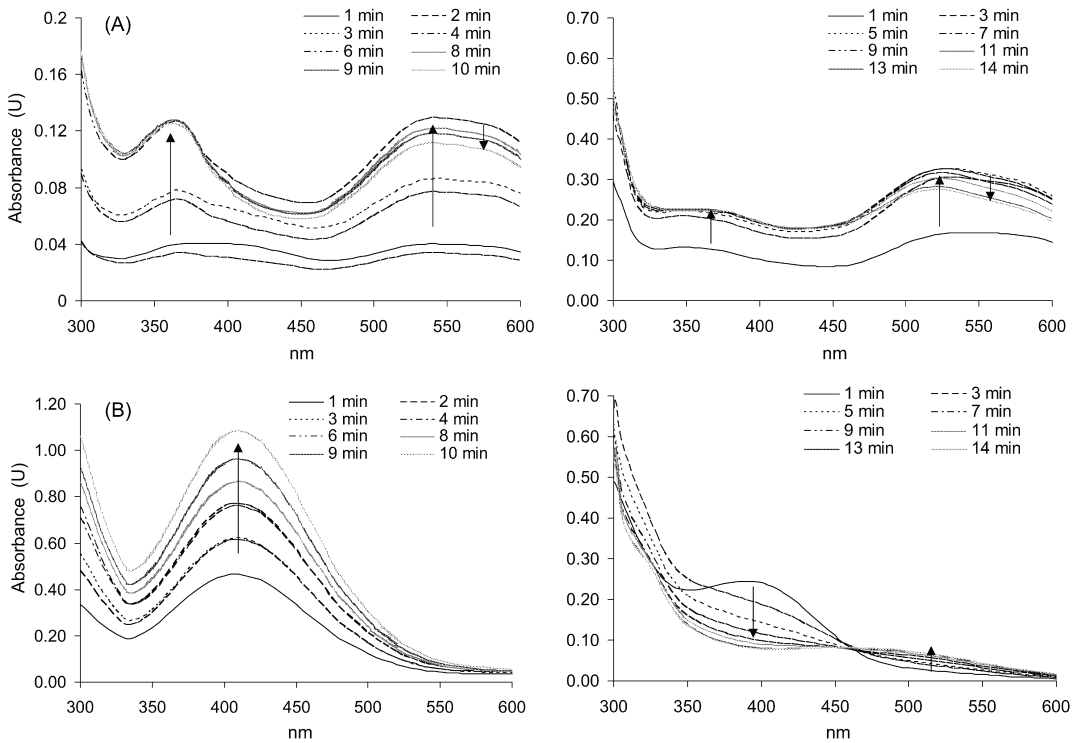

Fig. 2. Absorption product spectra from the oxidation of catechol (left side) and hydrocaffeic acid (right side) by TrT (A) and AbT (B). Absorption spectra of products shown as a function of reaction time.

2.5. ESR experiment

ESR experiment for semiquinone detection from the oxidation of the tripeptides, GGY, GYG and YGG, was performed on a Bruker EMX X-band ESR spectrometer equipped with an ER4119HS cavity (Bruker Analytische Messtechnik, Rheinstetten, Germany). The operating conditions were as follows: microwave power, 20 mW; modulation frequency, 100 kHz; field modulation amplitude, 0.2 G; receiver gain, 2×10^3; time constant, 2.56 ms; and conversion time, 2.56 ms. After initiation of the enzymatic reaction, reaction mixture was immediately transferred to an ESR flat cell, mounted within the ESR cavity, after which the measurement was started instantly. ESR signal appearance and disappearance was monitored as a function of time: one measurement, a sum of 34 successive scans, took 3.5 min, after which the ESR was restarted without a delay. GGY, GYG and YGG (2.5 mM) were dissolved in 0.2 M acetate buffer (pH 6.5) containing 0.05 M Zn^{2+}. Zn^{2+} was included in the reaction mixtures to stabilize the *o*-semiquinones [26]. Reactions were made at ambient temperature and in a volume of 0.5 ml. Dosing of the enzymes (0.55 nkat/mg peptide) was based on the determined activity of the enzymes on L-tyrosine (2 mM). To elucidate the effect of Zn^{2+} on the enzymatic activity, the oxidation of the peptides in presence of Zn^{2+} was also monitored by oxygen consumption measurement, and by following the UV–visible absorption spectrum formation during oxidation of the substrates.

3. Results

3.1. Product formation by TrT and AbT by determination of the UV–visible absorption spectrum

UV–visible absorption spectra of the oxidation products by TrT and AbT from different mono- and diphenolic compounds were measured. Based on the absorption spectra of product formation, specific wavelengths were established for determination of the kinetic constants K_m and V_{max} on the substrates. When catechol and hydrocaffeic acid were used as substrates, the UV–visible absorption spectrum obtained by TrT and AbT was completely different. AbT-catalyzed oxidation reaction led to an absorption maximum at 400 nm for both substrates, whereas in the TrT reactions the UV–visible absorption spectrum showed two maxima: one at 360 nm and another at 540–560 nm (Fig. 2). For the other substrates studied, the absorption spectra of the oxidation products of mono- and diphenolic compounds were similar between the enzymes. Tyrosinase-catalyzed oxidation products from phenol and phloretic acid, i.e. the corresponding monophenols for catechol and hydrocaffeic acid, with both enzymes resulted in absorption spectra similar to that of catechol and hydrocaffeic acid catalyzed by AbT, i.e. absorption maximum of product at 400 nm.

Table 1
Absorption maxima (nm) in the UV/Vis absorption spectrum of the primary product formation by TrT and AbT from the mono- and diphenolic substrates.

Substrate	Wavelength (nm)	
	TrT	AbT
L-Tyrosine	475	475
L-Dopa	475	475
p-Coumaric acid	360	360
Caffeic acid	480	480
L-Tyramine	475	475
L-Dopamine	475	475
Phloretic acid	400	400
Hydrocaffeic acid	530 (360)[a]	400
Phenol	390	390
Catechol	540 (360)[a]	400
p-Tyrosol	395	395

[a] Two products were detectable in TrT-catalyzed reactions. The absorption maximum of the second primary product is shown in parentheses.

Table 2
K_m (mM) and V_{max} (Abs/min) values of tyrosinases from TrT and AbT for mono- and diphenolic compounds, determined by spectrophotometric assay with substrate-specific wavelengths (Abs/nm).

Substrate	Detection absorbance (nm)	K_m (mM)		V_{max} (Abs/min)	
		TrT	AbT	TrT	AbT
L-Tyrosine	475	–	0.20	6[a]	13
L-Dopa	475	7.5	0.17	210	60
p-Coumaric acid	360	1.5	–	51	0
Caffeic acid	480	0.9	1.69	60	300
L-Tyramine	475	4.5	0.75	4	16
L-Dopamine	475	11	0.84	120	300
Phloretic acid	400	1.4	0.64	55	77
Hydrocaffeic acid	400/530[b]	3.0	0.91	450	840
Phenol	390	3.8	0.33	9	14
Catechol	400/540[c]	2.5	0.25	138	1500
p-Tyrosol	395	0.8	0.06	20	13

[a] Oxidation rate determined using tyrosine concentration of 2.5 mM, not the V_{max} value.
[b] Product formation followed at 400 and 530 nm with AbT and TrT, respectively.
[c] Product formation followed at 400 and 540 nm with AbT and TrT, respectively.

The absorption maxima selected for determining kinetic constants for the substrates were as follows: phenol 390 nm; catechol 400 (AbT) and 540 nm (TrT); *p*-coumaric acid 360 nm; caffeic acid 480 nm; L-tyramine, L-dopamine, L-tyrosine and L-dopa 475 nm; phloretic acid 400 nm; hydrocaffeic acid 400 (AbT) and 530 nm (TrT); and *p*-tyrosol 395 nm (Table 1).

3.2. Substrate specificity of TrT and AbT on mono- and diphenolic compounds

The ability of TrT and AbT to oxidize mono and diphenolic substrates with different substitution of carboxyl and amino groups was elucidated by determining the kinetic parameters, K_m and V_{max} (Table 2). The maximum reaction rate V_{max} is expressed as a change in absorbance as a function of time (Abs/min). The molar extinction coefficients (ε) for calculation of V_{max} (mol/s) and k_{cat} (s^{-1}) were not possible to determine. It was observed that different oxidation products were formed in the AbT and TrT catalyzed reactions. In addition, although the primary product from many substrates was same with both enzymes, different end products accumulated in TrT and AbT catalyzed reactions. For instance, in the oxidation of L-dopa, the dopachrome (λ_{max} at 475 nm) was the primary product with both enzymes, but with TrT the accumulation of dopachrome stopped, and other products accumulating at 370–460 nm appeared after initiating the reaction (data not shown).

The determined K_m values were approximately ten times lower for AbT than for TrT (Table 2). On the other hand, the maximum reaction rates V_{max} of corresponding mono- and diphenols varied between the enzymes depending on the substrates (Table 2). For instance, with L-dopa, V_{max} was clearly higher with TrT than AbT, whereas with caffeic acid and L-dopamine the outcome was opposite.

Under the conditions studied, AbT showed the highest affinity on monophenolic *p*-tyrosol (K_m 0.06 mM) and L-tyrosine (K_m 0.2 mM), and diphenolic L-dopa (K_m 0.17 mM) and catechol (K_m 0.25 mM). The highest K_m values for AbT were detected for caffeic acid, 1.61 mM and hydrocaffeic acid, 0.91 mM. Generally, AbT had higher affinity on monophenols than on the corresponding diphenols, except phenol, which showed slightly lower affinity when compared to catechol (Table 2). *p*-Coumaric acid was not oxidized by AbT. It was also seen that V_{max} was reached by AbT at certain substrate concentration with phenol, catechol, caffeic acid, phloretic acid, hydrocaffeic acid and *p*-tyrosol, above which the V_{max} began to decrease (data not shown). The decrease in the maximum reaction rate with increasing substrate concentrations is presumably related to inhibition of AbT by an excess of substrate.

TrT showed the highest affinity on *p*-tyrosol (K_m 0.8 mM), caffeic acid (K_m 0.9 mM), phloretic acid (K_m 1.4 mM) and *p*-coumaric acid (K_m 1.5 mM), whereas the affinity on L-dopamine (K_m 11 mM), L-dopa (K_m 7.5 mM) and L-tyramine (K_m 4.5 mM) was low (Table 2). The K_m value for L-tyrosine could not be determined due to insolubility of the substrate at concentrations above 2.5 mM. This concentration was not high enough to reach the V_{max} (Fig. 3). From the shape of the reaction rate *vs.* substrate concentration plot, the decrease in the maximum rate with increasing [S] was clearly seen in the TrT reactions with hydrocaffeic acid and caffeic acid, and also faintly with phloretic acid, referring to the inhibition of TrT by an excess of the substrate. Additionally, with catechol the corresponding substrate inhibition was detected for the product formation at 360 nm, but interestingly, not for the product formation at 540 nm (data not shown).

With monophenolic substrates a lag period prior to the oxidation reactions were detected by both enzymes. The lag periods for the oxidation reactions by AbT were longest with phenol (400 s), *p*-tyrosol (200–300 s) and L-tyrosine (200 s), with a substrate concentration of 15 mM (Table 3). The lag period increased as a function of substrate concentration for phenol, *p*-tyrosol and L-tyrosine, whereas for L-tyramine and phloretic acid the lag period decreased when substrate concentration was increased. The lag periods prior

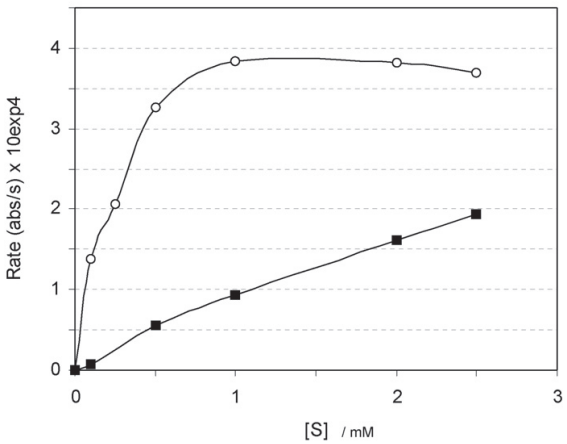

Fig. 3. Reaction rate as a function of substrate concentration [S], using L-tyrosine as substrate. Legends: AbT (○), TrT (■).

Table 3
Duration of lag periods (s) of tyrosinases from TrT and AbT for monophenolic compounds, determined by spectrophotometric assay.

Substrate	Detection absobance (nm)	Lag (s) with [S] 15 mM		Lag (s) with [S] 1 mM	
		TrT	AbT	TrT	AbT
L-Tyrosine	475	0[a]	200[a]	0–100[b]	50–100[b]
p-Coumaric acid	360	100–150	–	300	–
L-Tyramine	475	0	0	400	100–150
Phloretic acid	400	25–50	0–25	100–150	50–100
Phenol	390	200	400	500	300
p-Tyrosol	395	0	200–300	200	100–200

[a] Substrate concentration 2.5 mM.
[b] Substrate concentration 0.25 mM.

Table 4
Kinetic parameters of tyrosinases from TrT and AbT for the peptides GGY, GYG and YGG, determined by oxygen consumption measurement.

Enzyme	Substrate	V_{max} (mg L^{-1} s^{-1}) × 10^2	K_m (mM)	k_{cat} (s^{-1})	k_{cat}/K_m (s^{-1} mM^{-1})	Lag phase (s) with [S] 4 mM
TrT	Y		nd[a]			
TrT	GGY	11.9	3.1	7.2	2.4	120
TrT	GYG	6.9	3.9	4.2	1.1	120
TrT	YGG	5.2	6.0	3.2	0.5	120
AbT	Y		0.20			
AbT	GGY	2.7	0.11	3.0	26.5	600
AbT	GYG	2.8	0.18	3.1	17.1	240
AbT	YGG	3.6	0.21	4.0	19.0	180

[a] Could not be determined due to insolubility of the substrate.

to the oxidation of monophenols by TrT were longest with phenol (200 s), *p*-coumaric acid (100–150 s) and phloretic acid (25–50 s) with a substrate concentration of 15 mM (Table 3). Duration of the lag period decreased when substrate concentration increased with all of the tested monophenols in the TrT-catalyzed reactions.

3.3. Kinetic parameters for the tyrosine-containing tripeptides

The K_m and V_{max} values of AbT and TrT for the tripeptides varying in the position of tyrosine residue, GGY, GYG and YGG, were determined by an oxygen consumption assay. Similarly to the results obtained with mono- and diphenols, the K_m values of AbT for the peptides were over 10-fold lower than those of TrT (Table 4). AbT showed the highest apparent affinity on GGY (K_m 0.11 mM) and lowest on YGG (K_m 0.21 mM), whereas the highest catalytic efficiency k_{cat} was on YGG (4.0 s^{-1}) and lowest on GGY (3.0 s^{-1}). With YGG the affinity for AbT was rather similar to L-tyrosine (K_m 0.20 mM). TrT also showed the highest affinity on GGY (K_m 3.1 mM) and lowest on YGG (K_m 6 mM). However, contrary to AbT, the best catalytic efficiency was observed on GGY (7.2 s^{-1}) and lowest on YGG (3.2 s^{-1}). Interestingly, although there was a clear difference in K_m values, the k_{cat} values were relatively similar between AbT and TrT (Table 4). The lag periods prior to the oxidation reactions were shorter for TrT than AbT. The duration of the lag periods between the peptides was rather similar in the TrT-catalyzed reactions. However, the closer to the C-terminus the tyrosine residue was the longer

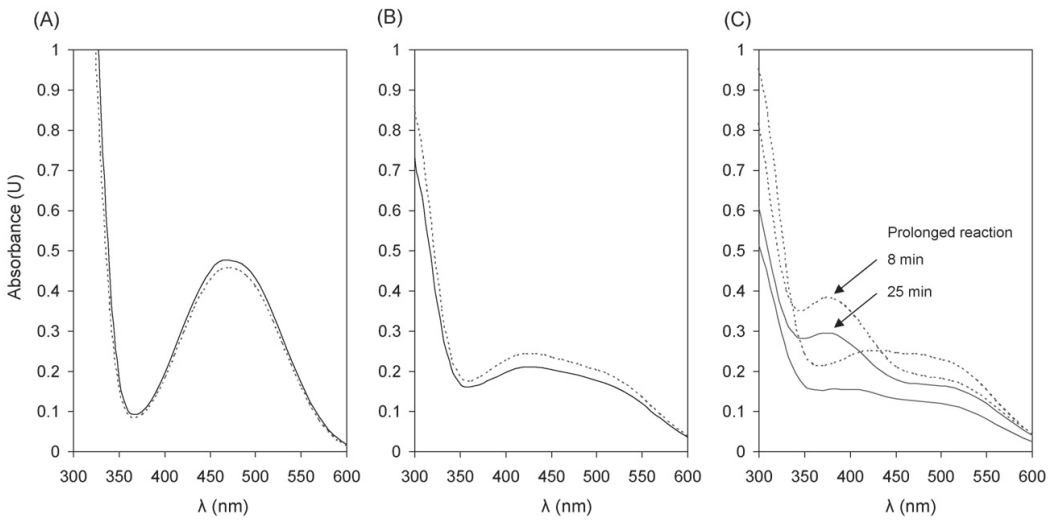

Fig. 4. Product spectra from the oxidation of the tripeptides YGG (A), GYG (B) and GGY (C) by TrT and AbT. Patterns: solid line for TrT, dashed line for AbT. In C arrows show the absorbance lines that represent prolonged reactions with TrT (at 8 min) and AbT (at 25 min), respectively.

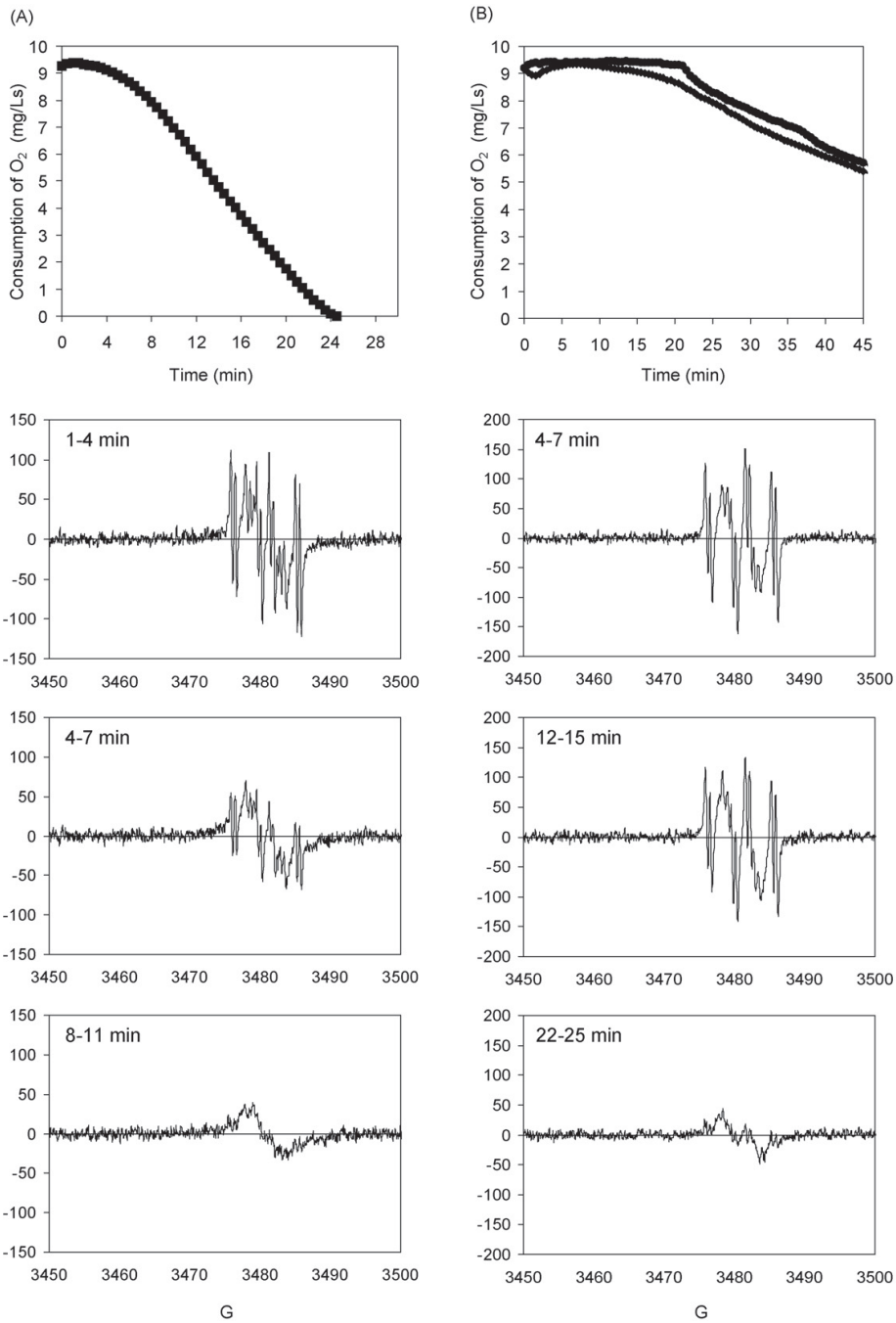

Fig. 5. Semiquinone-derived ESR signals and consumption of oxygen (mg L^{-1} s^{-1}) by TrT in presence of 1 mM GGY and GYG. Reaction conditions for oxygen consumption measurements correspond to the detection times of ESR signals as a function of reaction time. GGY (A) and GYG (B).

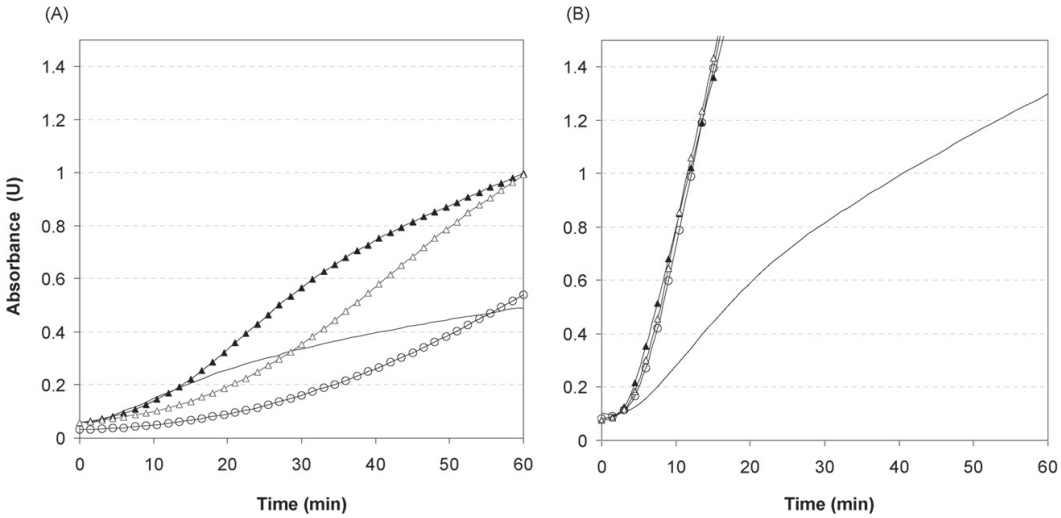

Fig. 6. Enzymatic activities of TrT and AbT on oxidation of L-dopa (15 mM) in presence of MBTH (0–10 mM). Formation rate for the MBTH-quinone adduct followed as an increase in absorbance at 510 nm as a function of time. Legends: MBTH concentration of 0 mM (−), 2.0 mM (△), 3.5 mM (○), 5.0 mM (▲).

the lag period was with AbT. The UV–visible absorption spectra for the oxidation products from the peptides were similar between the enzymes (Fig. 4). However, the product patterns differed clearly between the peptides. Oxidation product from YGG (Fig. 4A) corresponded to dopachrome-related product, showing a maximum at 475 nm, whereas with GYG (Fig. 4B) there was no clear absorption maximum and the product pattern was broad showing absorption maximum around 400–500 nm. Similarly with GGY the oxidation products gave broad absorption maximum at 400–500 nm. During a prolonged reaction (8 min for TrT, 25 min for AbT) absorption maximum with GGY shifted from 400–500 nm to 380 nm (Fig. 4C).

3.4. ESR measurements

Oxidation of GGY, GYG and YGG peptides by TrT and AbT was also monitored with ESR experiment in order to measure semiquinone radical production. The oxidation of the tripeptides GGY and GYG resulted in ESR spectra with two overlapping low intensity multiline ESR signals (Fig. 5A) by both enzymes (data on AbT not shown), corresponding to L-tyrosine-derived signal defined previously by Selinheimo et al. [20]. Signals were not detected by the enzymes or the substrates alone. Maximum signal intensities from GGY and GYG were relatively similar. When YGG was used as substrate, semiquinone-derived signal could not be detected in ESR. Oxidation of the tripeptides in the presence of Zn^{2+}, which was included in the reaction mixture to stabilize the semiquinones, was also monitored by an oxygen consumption assay (Fig. 5B) and by measuring the UV–visible absorption spectrum for the oxidation products (data not shown) in the conditions analogous to the ESR experiment. From the oxygen consumption measurements it was detected that the lag periods increased in presence of Zn^{2+} for all peptides and with both enzymes. With an oxygen consumption assay it was confirmed that the oxidation of YGG in presence of Zn^{2+} occurred by TrT and AbT (data not shown), although ESR signal was not detected from YGG. When the consumption of oxygen as a function of reaction time, and especially, the duration of the lag periods prior to the oxidation were compared to the appearance time of the semiquinone-derived signals, the outcome was unexpected. The semiquinone-derived ESR signal from GGY and GYG was observed to be present mainly during the lag period as detected by the oxygen consumption measurements (Fig. 5A and B). In other words, when the oxygen consumption was initiated, and thus, oxidation reaction accelerated, the ESR signal seemed to disappear. The result was also supported by the UV–visible absorption spectrum scanning measurements, monitored as a function of reaction time, in which the product formation accelerated when the ESR signal started to vanish (data not shown). However, some product formation was detected also during the lag period.

3.5. Effect of MBTH

Tyrosinase activity is often determined in presence of nucleophile MBTH, which is an efficient quinone binder [22–25]. Activities of TrT and AbT on L-dopa (15 mM) and L-tyrosine (2 mM) were determined in the presence of MBTH as well. Interestingly, when the monophenolase activities of AbT and TrT were determined using L-tyrosine in presence of MBTH, the lag period increased significantly as a function of MBTH concentration in the TrT-catalyzed reactions (Fig. 6A). On the other hand, with AbT the lag period was constant with varying MBTH concentrations (Fig. 6B). When the absorption spectra for the reaction products were determined on L-dopa and L-tyrosine in the presence of MBTH, absorbance intensity at 510 nm increased, referring to the MBTH-quinone adduct (data not shown). However, lowering the MBTH concentration a shift towards the dopachrome product (475 nm) was detected. For instance, when L-tyrosine was used as substrate, with MBTH concentration of $\leq$0.5 mM, a clear shift towards dopachrome was observed during the reaction with both enzymes. Apparently, with lower MBTH concentrations, not all of the formed quinones could be trapped.

4. Discussion

Detailed information on the substrate specificity of tyrosinases is essential for development of tyrosinase-based applications. The aim in the present study was to compare the substrate specificity of

the recently characterized tyrosinase TrT to the commercial tyrosinase preparation AbT. AbT is a well characterized enzyme, and for instance, the substrate specificity of AbT has been studied by Espín et al. [27,28], Fenoll et al. [29], Rodríguez-López et al. [30] and Xie et al. [31]. There is variation in the results of kinetic parameters for AbT, depending on both the level of purification of AbT and the assay method used [21,25–27]. Espín et al. [27] determined kinetic parameters by a spectrophotometric method using a purified AbT preparation, and reported for L-tyrosine a K_m value of 0.21 ± 0.01 mM, and for L-dopa a K_m value of 0.8 ± 0.04 mM. For the major isoform of AbT (Mw 43 kDa) Espín et al. [25] reported for L-tyrosine a K_m value of 0.021 ± 0.001 mM, and for L-dopa a K_m value of 0.038 ± 0.003 mM. Regarding hydrocaffeic acid (**4b**), Xie et al. [31] reported a K_m value of 1.24 mM for non-purified AbT, whereas Espín et al. [27] determined a K_m value of 1.89 mM for purified AbT. In the present work the experiments were made with the commercial AbT enzyme preparation, which has been reported to contain several isoforms of tyrosinase [13,14,31]. AbT was also further purified according to Duckworth and Coleman [21] for some of the experiments. For instance, the different location of tyrosine in the tripeptide, and its subsequent influence on the catalysis was studied with both crude and purified AbT, and the results were analogous (data not shown).

TrT and AbT showed notable differences in the affinity of the substrates studied. The K_m values for AbT were observed to be the highest for the substrates, in which an acid group was present in the structure (i.e. caffeic (**2b**) and hydrocaffeic acid (**4b**)). Furthermore, *p*-coumaric acid (**2a**) was not oxidized by AbT. It has been proposed that carboxylic aromatic structures can act as substrate analogues for tyrosinase, and they are believed to bind to both the *oxy*-form and the *met*-form of the coupled binuclear copper site [32–34]. Specifically *p*-coumaric acid and benzoic acid have been hypothesized to bind to the binuclear copper centre preferentially with the more acidic carboxylic group and compete with the substrate [32,34–37]. Rompel et al. [38] suggested that the blocking of active site could be based on either the coordination of the carboxylic group to the copper atoms or the binding of carboxylic acid group at a positively charged amino acid residue near the catalytic site. Since phloretic acid is oxidized by AbT, it has been suggested that particularly the conjugation of carboxylic group into the aromatic ring that is missing in phloretic acid is essential for binding of the acid group [32]. In contrast to AbT, TrT was observed to have clearly higher K_m values for substrates with amine substitution when compared to the substrates with carboxylic acid substitution. It appears particularly interesting that while AbT was not able to oxidize *p*-coumaric acid and showed the lowest affinity on caffeic acid among the tested substrates, TrT showed high affinity on caffeic acid and *p*-coumaric acid. Previously, Selinheimo et al. [17] reported for TrT the K_m values of 1.3, 1.6 and 3.0 mM for *p*-tyrosol, *p*-coumaric acid and L-dopa, respectively, determined by monitoring consumption of oxygen which differ to some extent from the K_m values of the present study, assayed by a spectrophotometric method.

The negative effect of proximity of an amine group on TrT was also detected in the K_m values of the tripeptides, as the highest K_m value and lowest catalytic efficacy (k_{cat}) was on YGG, in which tyrosine residue is in the amino-terminal end of the peptide. With AbT the lowest K_m value was detected, when the tyrosine residue located in the carboxyl-terminal end, i.e. for the GGY tripeptide. However, with GGY the k_{cat} was the lowest and the lag period longest for AbT, suggesting high affinity, but poorer catalytic efficacy as compared to the other peptides. Although the exact reasons for the differences in the K_m values between TrT and AbT remain to be resolved, it could be that the coordinating amino acids of enzymes, which assist substrates to the active site, differ between the enzymes. Hence, varying polarity and acidity of the phenolic hydroxyl group of the substrate could cause different orientation of the substrate to the active site of AbT and TrT. Determining the tertiary structure of AbT and TrT and the detailed construction of active site is essential to elicit the explanation for the result.

The activity assay using a nucleophilic quinone binder MBTH has been reported to be relatively sensitive and accurate for determining tyrosinase activity, as with this nucleophile a relatively stable quinone adduct can be formed [22–25]. It has also been reported that the lag period, which is typically present in the tyrosinase-catalyzed monophenol oxidation, could be shortened by using nucleophilic coupling reactions through quick generation of *o*-diphenols [23]. During the lag period, the *oxy*-form of tyrosinase, which is capable for the hydroxylation of monophenols, is generated by indirect *o*-diphenol formation from the *met*-form of tyrosinase, which can perform only the oxidation of diphenols [7,39]. In the TrT-catalyzed reactions with L-tyrosine and MBTH, the duration of the lag period was unexpectedly increased as a function of MBTH concentration, referring that MBTH retarded the initiation of the catalytic cycle by TrT. However, the maximum reaction rate was not significantly changed by MBTH. Hence, it seemed that MBTH retarded principally the transformation of TrT from the *met*- to the *oxy*-form. With AbT the effect of MBTH was as reported previously [24,25]: the lag was constant and even decreased when compared to the reactions without MBTH.

The lag periods for TrT and AbT were measured for all the monophenolic substrates studied (without MBTH). It has been proposed that a monophenolic substrate with high affinity saturates the *met*-form of enzyme [25]. Hence, if most of the enzyme is in a form, in which monophenols are bound to the *met*-tyrosinase, the transformation from the *met*- to the *oxy*-form is delayed because there is less free enzyme for diphenol oxidation. Espín et al. [25] reported that lag period increased when substrate concentration ([S]) was increased, suggesting that the *met*-form of the enzyme was increasingly saturated with monophenol when [S] was increased. When the lag periods were monitored in the AbT-catalyzed reactions, the lag period increased as a function of [S] with *p*-tyrosol, L-tyrosine and phenol, but with L-tyramine and phloretic acid the situation was opposite. On the other hand, with TrT, the lag period was invariably shortened with increasing [S]. However, the K_m values for TrT were relatively high which might partly explain the lag durations. If the reactions with lower [S] were still clearly beyond V_{max}, the lag could be expected to increase by increasing [S], as with lower [S] there is not enough substrate to occupy the active site. This might also partly explain the incoherence in the duration of the lag periods with AbT, as L-tyramine and phloretic acid, which showed decreasing lag with increasing [S], were also the substrates with highest K_m values. However, the difference between the K_m values was not very significant between the substrates with different changes in lag duration, suggesting that there are also other factors behind.

The product formation in the tyrosinase catalysis was determined by monitoring the changes in UV–visible absorption spectrum as a function of reaction time. Unpredictably, diphenols catechol (**5b**) and hydrocaffeic acid (**4b**) gave different product pattern by AbT and TrT, whereas the products from the corresponding monophenols (phenol (**5a**) and phloretic acid (**4a**)) did not differ between the enzymes. The dissimilarity in the diphenol catalysis between the enzymes seemed to be specific only for these substrates, as for the other diphenols studied, i.e. L-dopa, L-dopamine and caffeic acid, the product spectrum was similar between the enzymes. Although there is not clear explanation for the found differences in the oxidation products from catechol and hydrocaffeic acid, it could be hypothesized that the observations could

relate to the differences of the enzymes in their affinity to the non-enzymatic quinone-derived products. It is known that the quinones formed in the catalysis will quickly react further and also act as substrates for tyrosinase. Typically oxidation of catechol by tyrosinases is known to generate products absorbing at 390–400 nm [40], which was also detected with AbT. Interestingly these products were not detected with TrT. It could be anticipated that TrT immediately further oxidized the product resulting from the non-enzymatic reactions of *o*-quinone. Hence, the primary product at 390–400 nm could not have accumulated in the TrT-catalyzed reactions.

When enzymatic oxidation of tripeptides was examined, the position of tyrosine residue in the tripeptide was observed to influence differently on the TrT- and AbT-catalyzed reactions. The reaction products were different depending on whether the tyrosine was located in the carboxyl- or amino-terminus or in the middle of the peptide; however, differences in the reaction products between AbT and TrT were not detected. Land et al. [41,42] have shown that increasing the chain length of catecholamines leads to unachievable cyclization of these amines due to a steric hindrance. Based on the product accumulation from the tripeptides GGY, GYG and YGG by the tyrosinases, only oxidation of YGG was observed to lead to the formation of dopachrome-type cyclization product. Probably in the case of GGY and GYG, cyclization of peptide via reaction of quinone with nucleophilic amine was unfavourable due to the steric hindrance. When the semiquinone radical formation during the oxidation of the peptides was studied by ESR, Zn^{2+} was included in the reaction solution to stabilize the semiquinones [26]. Zn^{2+} was observed to influence on the oxidation readiness of the peptides by lengthening the lag phase prior to the oxidation. The presence of transition metal ions, such as Zn^{2+}, has been reported to affect the lag period related to oxidation of monophenols either by prolonging or by diminishing the lag phase [43–45]. The transition metal ions can also affect the chemical properties of melanins formed by the tyrosinase-catalyzed oxidation of L-dopa. Particularly, the non-carboxylative rearrangement of dopachrome to 5,6-dihydroxyindole-2-carboxylic acid may occur in the presence of metal ions [46–48]. In actual fact, the UV–visible absorption spectra on the oxidation products of the tripeptides clearly changed in presence of Zn^{2+}. With YGG an absorption maximum was at 430 nm instead of 475 nm, and with GYG and GGY the maximum was around 300–450 nm (data not shown). Unexpectedly, semiquinone-derived ESR signal was not detected for YGG oxidation by the tyrosinases. This could be due to the inability of Zn^{2+} to stabilize the YGG-derived oxidation product, which differed from that of GGY and GYG.

Based on the results of the oxygen consumption of the tripeptides by AbT and TrT in presence of the Zn^{2+}, the ESR signal was noted to appear during the lag period, and disappear when the oxidation reaction accelerated. The results clearly indicate that the semiquinone-derived ESR signal was present in the very beginning of the catalysis. However, after indirect generation of diphenols during enzymatic catalysis, semiquinones should be detectable due to auto-oxidation. After formation of quinines, semiquinones are generated by inverse disproportionation between diphenol and quinone [49]. Because in this study the semiquinone-derived ESR signals were mostly detected during the lag period, it is intriguing to suggest that the semiquinone formation relates specifically to the reaction catalyzed by the *met*-form of tyrosinase.

5. Conclusions

The extracellular fungal tyrosinase TrT and the intracellular tyrosinase AbT were found to clearly differ in their substrate specificity. The product pattern from catechol and hydrocaffeic acid was also observed to be different between these enzymes. Although the detailed catalytic mechanisms of the enzymes are still to be explicated, the noted contrasts in the determined K_m values for the substrates could suggest differences in the distribution of acid/base residues and orientation of the substrates in the active site of TrT and AbT.

Acknowledgements

This paper has been carried out with financial support from the Research Foundation of Raisiogroup (Raisio, Finland), the Consortium Cresci belonging to University of Perugia (Italy), and the STReP-project (HIPERMAX/NMP-3-CT-2003-505790) funded by the European Commission; the contents of the publication reflects only the views of the authors. Dr. Markku Saloheimo is acknowledged for the expression construct for TrT production, BSc. Michael Bailey for the TrT production, and Heljä Heikkinen for technical assistance.

References

[1] Lerch K, Huber M, Schneider H, Drexel R, Linzen B. Different origins of metal binding sites in binuclear copper proteins, tyrosinase and hemocyanin. J Inorg Biochem 1986;26:213–7.
[2] Lerch K. *Neurosopra* tyrosinase: structural, spectroscopic and catalytic properties. Mol Cell Biochem 1983;52:125–38.
[3] Robb DA. Tyrosinase. In: Lontie R, editor. Copper proteins and copper enzymes. Boca Raton, FL: CRC Press Inc.; 1984. p. 207–40.
[4] Jolley RL, Evans LH, Mason HS. Reversible oxygenation of tyrosinase. Biochem Biophys Res Commun 1972;46:878–84.
[5] Makino N, Mason HS. Reactivity of oxytyrosinase towards substrates. J Biol Chem 1973;248:5731–5.
[6] Jolley RL, Evans LH, Makino N, Mason HS. Oxytyrosinase. J Biol Chem 1974;249:335–45.
[7] Solomon EI, Sundaram UM, Machonkin TE. Multicopper oxidases and oxygenases. Chem Rev 1996;96:2563–606.
[8] Matoba Y, Kumagai T, Yamamoto A, Yoshitsu H, Sugiyama M. Crystallographic evidence that the dinuclear copper center of tyrosinase is flexible during catalysis. J Biol Chem 2006;281:8981–90.
[9] Klabunde T, Eicken C, Sacchettini JC, Krebs B. Crystal structure of a plant catechol oxidase containg a dicopper center. Nat Struct Biol 1998;5:1084–90.
[10] Cuff ME, Miller KI, van Holde KE, Hendrickson WA. Crystal structure of a functional unit from *Octopus dofleini hemocyanin*. J Mol Biol 1998;278:855–70.
[11] Decker H, Schweikardt T, Tuczek F. The first crystal structure of tyrosinase: all questions answered? Angew Chem Int Ed 2006;45:4546–50.
[12] Marusek CM, Trobaugh NM, Flurkey WH, Inlow JK. Comparative analysis of polyphenol oxidase from plant & fungal species. J Inorg Biochem 2006;100:108–23.
[13] Wichers HJ, Gerritse YA, Chapelon CGJ. Tyrosinase isoforms from the fruitbodies of *Agaricus bisporus*. Phytochemistry 1996;43:333–7.
[14] Wichers HJ, Recourt K, Hendriks M, Ebbelaar CEM, Biancone G, Hoeberichts FA, et al. Cloning, expression and characterisation of two tyrosinase cDNAs from *Agaricus bisporus*. Appl Microbiol Biotechnol 2003;61:336–41.
[15] Nakamura T, Sho S, Ogura Y. On the purification and properties of mushroom tyrosinase. J Biochem 1966;59:481–6.
[16] Robb DA, Gutteridge S. The polypeptide composition of two fungal tyrosinases. Phytochemistry 1981;20:1481–5.
[17] Selinheimo E, Saloheimo M, Ahola E, Westerholm-Parvinen A, Kalkkinen N, Buchert J, et al. Production and characterization of a secreted, C-terminally processed tyrosinase from the filamentous fungus *Trichoderma reesei*. FEBS J 2006;273:4322–35.
[18] Leu W, Chen L, Liaw L, Lee Y. Secretion of the *Streptomyces* tyrosinase is mediated through its trans-activator. MelC J Biol Chem 1992;267:20108–13.
[19] Tsai TT, Lee YH. Roles of copper ligands in the activation and secretion of *Streptomyces* tyrosinase. J Biol Chem 1998;273:19243–50.
[20] Selinheimo E, NiEidhin D, Steffensen C, Nielsen J, Lomascolo A, Halaouli S, et al. Comparison of the characteristics of fungal and plant tyrosinases. J Biotechnol 2007;130:471–80.
[21] Duckworth HW, Coleman JE. Kinetic properties of mushroom tyrosinase. J Biol Chem 1970;245:1613–25.
[22] Rodríguez-López JN, Escribano J, Garcia-Canovas F. A continuous spectrophotometric method for the determination of monophenolase activity of tyrosinase using 3-methyl 2-benzothiazolinone hydrazone. Anal Biochem 1994;216:205–12.
[23] Espín JC, Morales M, Varón R, Tudela J, García-Cánovas F. A continuous spectrophotometric method for determining the monophenolase and diphenolase activities of apple polyphenol oxidase. Anal Biochem 1995;231:237–46.

[24] Espín JC, Morales M, García-Ruiz PA, Tudela J, García-Cánovas F. Improvement of a continuous spectrophotometric method for determining the monophenolase and diphenolase activities of mushroom polyphenol oxidase. J Agric Food Chem 1997;45:1084–90.
[25] Espín JC, Jolivet S, Wichers HJ. Kinetic study of the oxydation of γ-L-glutaminyl-4-hydroxybenzene catalyzed by mushroom (*A. bisporus*) tyrosinase. J Agric Food Chem 1999;47:3495–502.
[26] Yamasaki H, Grace SC. EPR detection of phytophenoxyl radicals stabilized by zinc ions: evidence for the redox coupling of plant phenolics with ascorbate in the H_2O_2-peroxidase system. FEBS Lett 1998;422:377–80.
[27] Espín JC, García-Ruiz PA, Tudela J, García-Cánovas F. Study of stereospecificity in mushroom tyrosinase. Biochem J 1998;331:547–51.
[28] Espín JC, Varon R, Fenoll LG, Gilabert MA, Garcia-Ruiz PA, Tudela J, et al. Kinetic characterization of the substrate specificity and mechanism of mushroom tyrosinase. Eur J Biochem 2000;267:1270–9.
[29] Fenoll LG, Rodriguez-Lopez JN, Garcia-Molina F, Garcia-Canovas F, Tudela J. Michaelis constants of mushroom tyrosinase with respect to oxygen in the presence of monophenols and diphenols. Int J Biochem Cell B 2002;34:332–6.
[30] Rodríguez-López JN, Fenoll LG, García-Ruiz PA, Varón R, Tudela J, Thorneley RN, et al. Stopped-flow and steady-state study of the diphenolase activity of mushroom tyrosinase. Biochemistry 2000;39:10497–506.
[31] Xie J-J, Song K-K, Qiu L, He Q, Huang H, Chen Q-X. Inhibitory effects of substrate analogues on enzyme activity and substrate specificities of mushroom tyrosinase. Food Chemistry 2007;103:1075–9.
[32] Fan Y, Flurkey WH. Purification and characterization of tyrosinase from gill tissue of Portabella mushroom. Phytochemistry 2004;65:671–8.
[33] Lim JY, Ishiguro K, Kubo I. Tyrosinase inhibitory *p*-coumaric acid from ginseng leaves. Phytother Res 1999;13:371–5.
[34] Kubo I, Nihei K, Tsujimoto K. Methyl *p*-coumarate, a melanin formation inhibitor in B16 mouse melanoma cells. Bioorg Med Chem 2004;12:5349–54.
[35] Conrad JS, Dawson SR, Hubbard ER, Meyers TE, Strothkamp KG. Inhibitor binding to the binuclear active site of tyrosinase: temperature, pH, and solvent deuterium isotope effects. Biochemistry 1994;33:5739–44.
[36] Winkler ME, Lerch K, Solomon EI. Competitive inhibitor binding to the binuclear copper active site in tyrosinase. J Am Chem Soc 1981;103:7001–3.
[37] Wilcox DE, Porras AG, Hwang YT, Lerch K, Winkler ME, Solomon EI. Substrate analogue binding to the coupled binuclear copper active site in tyrosinase. J Am Chem Soc 1985;107:4015–27.
[38] Rompel A, Fischer H, Meiwes D, Buldt-Karentzopoulos K, Magrini A, Eicken C, et al. Substrate specificity of catechol oxidase from *Lycopus europaeus* and characterization of the bioproducts of enzymic caffeic acid oxidation. FEBS Lett 1999;445:103–10.
[39] Cooksey CJ, Garratt PJ, Land EJ, Pavel S, Ramsden CA, Riley PA, et al. Evidence of the indirect formation of the catecholic intermediate substrate responsible for the autoactivation kinetics of tyrosinase. J Biol Chem 1997;272:26226–35.
[40] Mason H. The chemistry of melanin. VI. Mechanism of the oxidation of catechol by tyrosinase. J Biol Chem 1949;181:803–12.
[41] Land EJ, Ramsden CA, Riley PA. Quinone chemistry and melanogenesis. Methods Enzymol 2004;378:88–109.
[42] Land EJ, Ramsden CA, Riley PA, Yoganathan G. Formation of *para*-quinomethanes *via* 4-aminobutylcatechol oxidation and *ortho*-quinone tautomerism. Org Biomol Chem 2003;1:3120–4.
[43] Palumbo A, Misuraca G, d'Ischia M, Prota G. Effect of metal ions on the kinetics of tyrosine oxidation catalysed by tyrosinase. Biochem J 1985;228:647–51.
[44] Ros JR, Rodríguez-López JN, Garcia-Cánovas F. Effect of ferrous ions on the monophenolase activity of tyrosinase. Biochim Biophys Acta 1993;1163:303–8.
[45] Sánchez-Ferrer A, Rodríguez-López JN, García-Cánovas F, García-Carmona F. Tyrosinase: a comprehensive review of its mechanism. Biochimica et Biophysica Acta 1995;1247:1–11.
[46] Bowness JM, Morton RA. The association of zinc and other metals with melanin and melanin-protein complex. Biochem J 1953;53:620–6.
[47] Palumbo A, d'Ischia M, Misuraca G, Prota G. Effect of metal ions on the rearrangement of dopachrome. Biochim Biophys Acta 1987;925:203–9.
[48] Palumbo A, d'Ischia M, Misuraca G, Prota G, Schultz TM. Structural modifications in biosynthetic melanins induced by metal ions. Biochim Biophys Acta 1988;964:193–9.
[49] Kalyanaraman B. Characterization of *o*-semiquinone radicals in biological systems. Methods Enzymol 1990;186:333–43.